1 Engineering colloidal quantum dots

Synthesis, surface chemistry, and self-assembly

Maryna I. Bodnarchuk and Maksym V. Kovalenko

1.1 Colloidal synthesis of inorganic nanocrystals and quantum dots

1.1.1 Introductory remarks: history and terminology

Historically, one of the most accomplished nanoscale building blocks is the quantum dot, also known as a semiconductor nanocrystal (NC). Since the early 1980s, the chemistry of colloidal nanostructures has been almost exclusively concentrated on colloidal semiconductors such as CdS and TiO_2. Those early efforts rose from the oil crisis in the late 1970s, and semiconductor NCs with enhanced surface chemistry were considered highly important for efficient harvesting of solar energy via photoelectrochemistry [1] and later using dye-sensitized solar cells [2]. The interest in quantum dots was further triggered by the discovery of quantum-size effects in the optical spectra of nanometer-sized semiconductors, by the teams of A. Ekimov and A. Efros in the USSR [3, 4], and by L. Brus at Bell Laboratories in the USA [5]. The first observations were collected from optical measurements on the semiconductor dots dispersed in glass matrices [3] or aqueous semiconductor sols [5]. Until the mid-1990s, a major challenge was to master the production of quantum dots in the form of uniform, size-tunable and isolable NCs, with adjustable physical and chemical properties. This goal was largely accomplished only in 1993 when the hot-injection technique was introduced by Murray, Norris, and Bawendi, enabling synthesis of highly monodisperse Cd chalcogenide NCs [6]. Surfactant-assisted nucleation and growth in organic solvents, initiated by hot-injection [6] or by heating [7] the reaction mixture became standard for growing monodisperse colloidal NCs of metals, metal oxides, and other classes of inorganic compounds. Even water was demonstrated as a suitable synthesis medium for certain compounds, such as thiol-capped II–VI semiconductor NCs [8] with bright and stable photoluminescence.

The multitude of methods for producing nanosize particles and crystals is truly impressive (Figure 1.1). The top-down approaches for the formation of engineered nanomaterials include fragmentation and structuring of macroscopic solids, either mechanically (e.g., ball-milling) or chemically (lithography, exfoliation, etching, etc.). The bottom-up assembly starts with molecules, atoms, and ions and proceeds via gas-phase or liquid-phase chemical reactions, aggregation, and crystallization. Liquid-phase synthesis in aqueous or non-aqueous solvents turned out to be particularly convenient and successful.

Colloidal Quantum Dot Optoelectronics and Photovoltaics, eds. G. Konstantatos and E. H. Sargent.
Published by Cambridge University Press.

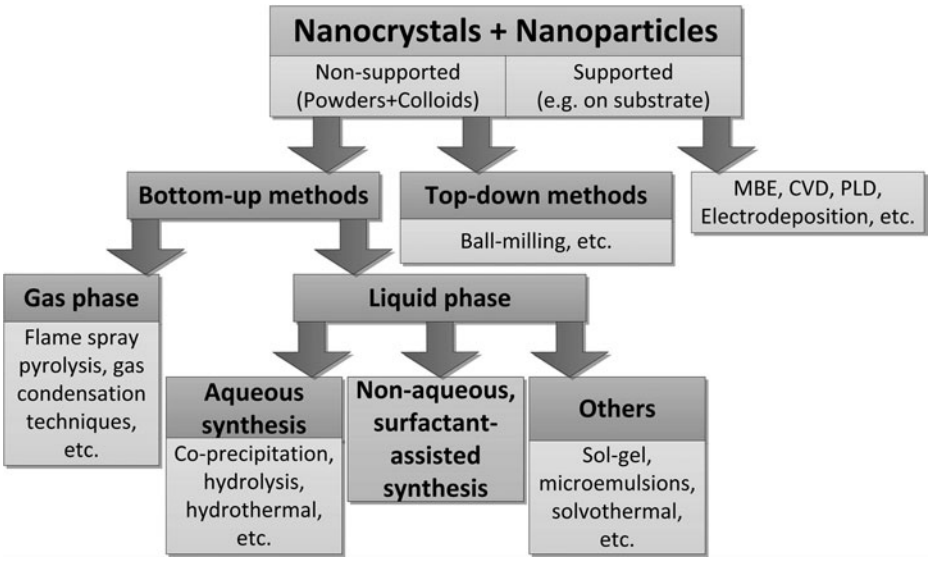

Figure 1.1 An overview of various methods for fabrication of inorganic nanoparticles and nanocrystals. Non-aqueous surfactant-assisted synthesis is colloidal synthesis in organic solvents – the key methodology for all NC quantum dots discussed in this book. Color version of this figure is available online at www.cambridge.org/9780521198264.

Surfactant-assisted, colloidal synthesis in organic solvents earned the highest appreciation and will be discussed here in detail. Physical and chemical methods of growth on planar supports constitute a separate and broad field of science and technology, outside the scope of this book.

While the general term "nanoparticle" refers to the characteristic size (usually 1–100 nm), a *crystalline* nanoparticle is often called a "nanocrystal" (Figure 1.2(a), (b)). The quantum-mechanical definition of "quantum dot" refers to the peculiar electronic structure – the piece of matter (typically a semiconductor) having electrons and holes confined in all three dimensions. When this property is found in a NC, that entity is often called a "NC quantum dot". For simplicity, the terms "semiconductor NC" and "quantum dot" are used interchangeably, a legitimate assumption for most of 2–20 nm NCs. Finally, the phrases "colloidal NCs" or "colloidal quantum dots" indicate the colloidal method of synthesis and colloidal state of dispersion (Figure 1.2(c)).

1.1.2 Basics of the surfactant-assisted colloidal synthesis of NC quantum dots

In a typical NC synthesis (Figure 1.2(c), (d) and Figure 1.3), suitable molecular precursors are introduced into a reaction mixture, where they undergo a chemical reaction supplying "monomers" (reaction I) for the homogeneous nucleation of NCs (reaction II). The further growth occurs due to continuous flux of monomers onto the NC surface (reaction III). Upon depletion of the monomer concentration, further growth may occur through the Ostwald ripening process (also known as Lifshitz–Slyozov–Wagner growth) [10, 11], i.e., growth of larger dots by dissolving smaller ones. All these consecutive stages can be significantly altered by the presence of surface capping molecules, also

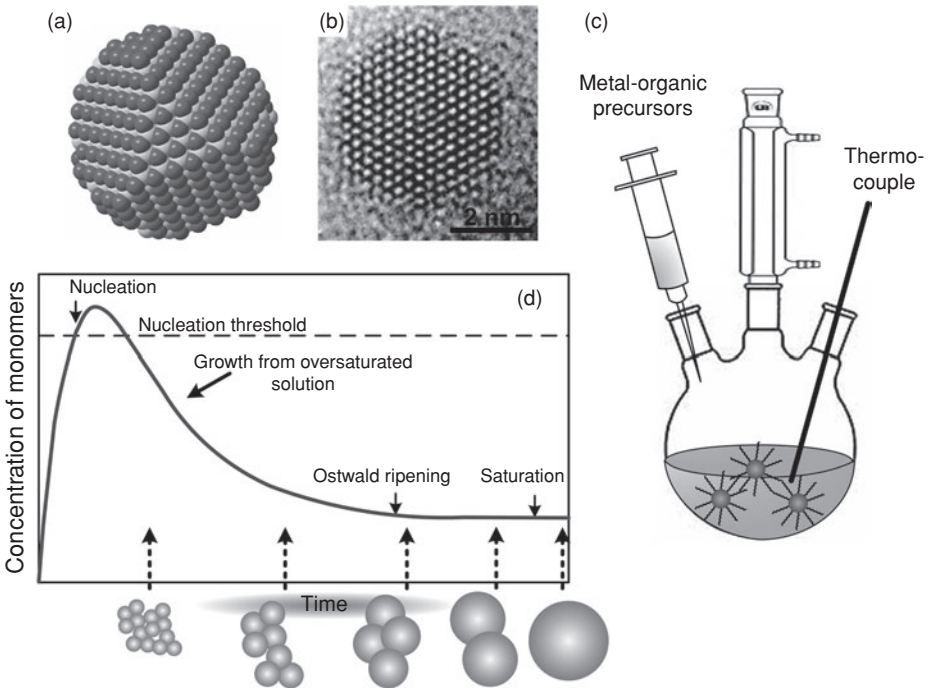

Figure 1.2 Colloidal NC quantum dots. (a) Crystallographic model and (b) high-resolution TEM image of a single CdSe NC. Reproduced with permission from [9]. (c) Illustration of a typical setup used in the chemical synthesis of colloidal NCs. (d) Schematics of the main stages in the synthesis of colloidal NCs in relation to the concentration of the monomers. Color version of this figure is available online at www.cambridge.org/9780521198264. Adapted from [9].

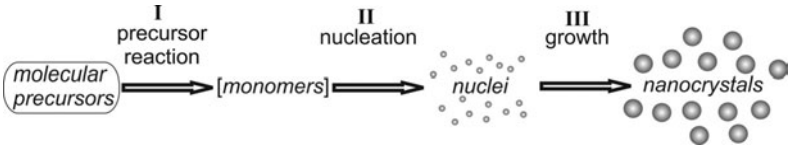

Figure 1.3 Illustration of the three key steps in the synthesis of colloidal NCs: precursor-to-monomer conversion, homogeneous nucleation, and heterogeneous growth.

known as surfactants or stabilizers. These molecules dynamically adhere to the NC surface during NC nucleation and growth, and provide chemical and colloidal stability of the final product. It is generally accepted that temporal separation of the nucleation and growth is required for growing monodisperse NCs [6, 12]. The concept of the nucleation "burst" relates to the fast nucleation that occurs after the monomer concentration surpasses a certain threshold, as originally proposed by La Mer and others (Figure 1.2(d)) [12, 13]. Fast nucleation is best implemented using the so-called *hot-injection technique*, in which the precursors are rapidly injected into a hot solvent to induce their fast conversion into monomers (Figure 1.2(c)) [6, 14]. Alternatively, the separation of nucleation and growth stages can be achieved upon steady heating of the reaction mixture if the initial accumulation of monomers is sufficiently slow [15]. High-boiling solvents are typically used to provide a wide reaction temperature window of 25–350 °C.

Studies have demonstrated the great importance of the optimal precursor chemistry. High reactivity of precursors is the basis of the hot-injection technique. In the framework of the classical nucleation theory the nucleation rate *dN/dt* is expressed as [16]:

$$\frac{dN}{dt} = A \exp\left(-\frac{\Delta G^N}{RT}\right),$$

where $\Delta G^N = 16\pi\gamma^3 V_m^2/3(RT \ln S)^2$ is the activation free energy, γ is the specific surface energy, V_m is the molar volume, and S is the supersaturation. The last is defined as the ratio between the monomer concentration and the solubility of the bulk material: $S = [\text{Monomer}]/C^o_{bulk}$. Hence the decomposition of precursors must generate a large concentration of monomers in a short period of time (typically during the first 0.1–10 s) at a given reaction temperature. Excellent examples of highly reactive precursors are metal amides which show excellent results in the synthesis of metallic Co [17], Fe [18], FeCo [19] NCs and metal compound NCs such as SnTe [20], SnS [21], SnSe [22], PbSnTe [23], $Fe_{1-y}O$ [24], and γ-Fe_2O_3 [25] NCs. Much safer, cheaper, and less air-sensitive are metal carboxylates, which are routinely used in the preparation of Pb chalcogenide [26, 27], Cd chalcogenide [28, 29], and many other NCs. Schemes (1)–(8) below illustrate various chemical reactions underlying the synthesis of inorganic NCs. Trimethysilyl-, alkyl-, and trialkylphosphine-based derivatives are often used as non-metal precursors. At the same time, the procedures developed more recently involve simple, inexpensive, and safe inorganic precursors such as metal chlorides and elemental substances (schemes (4) and (6)), providing NCs of comparable quality. Typical stabiliziers (surfactants or capping ligands) include long-chain carboxylic and phosphonic acids (e.g., oleic acid, OA, myristic acid, MA, and n-octadecylphosphonic acid, ODPA), alkylthiols (e.g., dodecanethiol), alkyl phosphines and alkylphosphine oxides (typically trioctylphosphine, TOP, and trioctylphosphine oxide, TOPO), and alkylamines such as hexadecylmine (HDA). If the stabilizer can act as a solvent, such as HDA or TOPO, it is called a coordinating solvent. Alternatively, a chemically inert, non-coordinating solvent is used (e.g., octadecene, ODE).

$$Bi[N(SiMe_3)_2]_3 \xrightarrow{140\,^\circ C,\ HDA,\ LiBH(Et)_2} Bi\ NCs,\ [30] \quad (1)$$

$$Sn[N(SiMe_3)_2]_2 + (C_8H_{17})_2Te \xrightarrow{140\,^\circ C,\ TOP-HDA} SnTe\ NCs,\ [20] \quad (2)$$

$$Pb(CH_3COO)_2 + [Me_3Si]_2S \xrightarrow{180\,^\circ C,\ oleic\ acid} PbS\ NCs,\ [27] \quad (3)$$

$$PbCl_2 + S \xrightarrow{150\,^\circ C,\ OLA} PbS\ NCs,\ [27, 31] \quad (4)$$

$$Cd(CH_3)_2 + (C_8H_{17})_3PSe \xrightarrow{300\,^\circ C,\ HDA-TOPO-TOP} CdSe\ NCs,\ [32] \quad (5)$$

$$Cd(C_{13}H_{27}COO)_2 + Se \xrightarrow{260\,^\circ C,\ TOP} CdSe\ NCs,\ [29] \quad (6)$$

$$InCl_3 + [Me_3Si]_3P \xrightarrow{260\,^\circ C,\ TOP} InP\ NCs,\ [33] \quad (7)$$

$$In(CH_3COO)_3 + PH_3 \xrightarrow{260\,^\circ C,\ ODE-MA} InP\ NCs,\ [34] \quad (8)$$

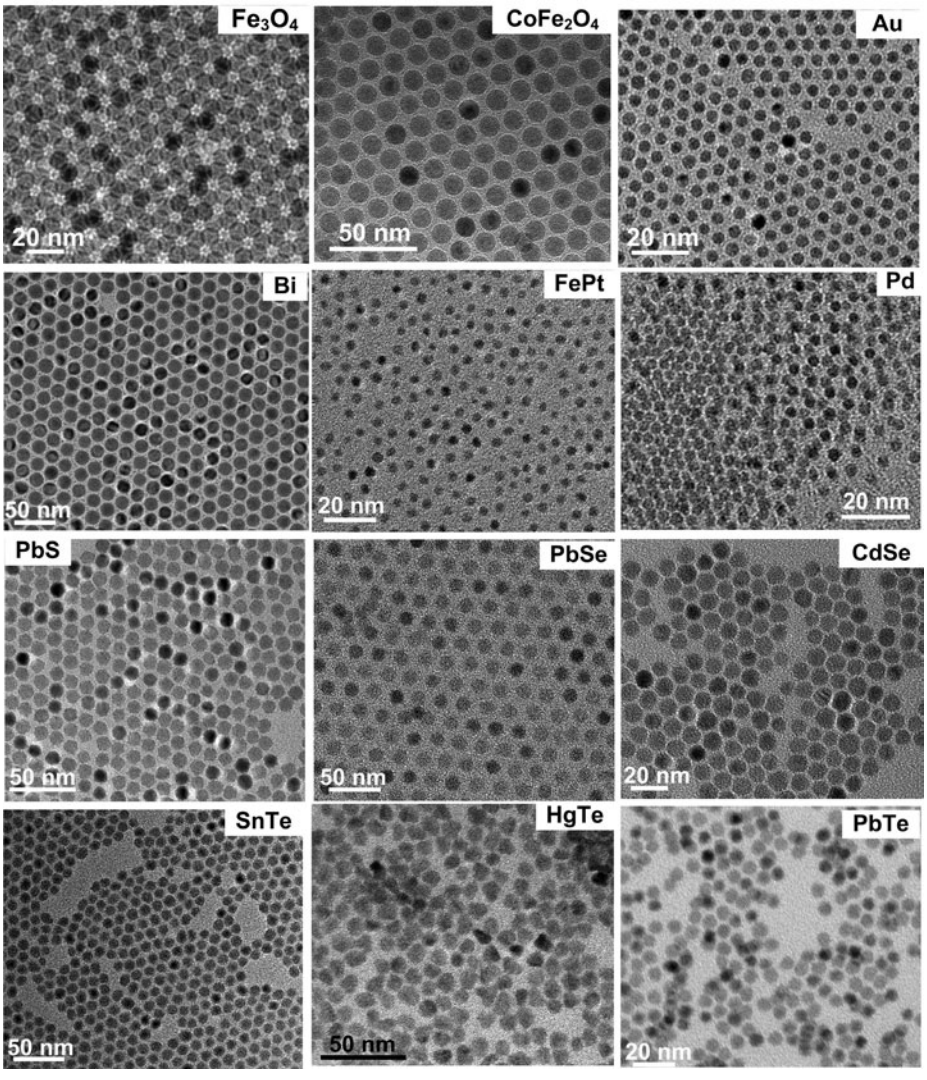

Figure 1.4 Typical examples of monodisperse, colloidally synthesized inorganic NCs.

The synthesis of monodisperse NCs has been developed for II–VI (CdSe, CdTe, CdS) [6, 28, 32], III–V (InP, InAs) [33, 35] and IV–VI (PbS, PbSe, PbTe) [26, 27, 31, 36] NCs. A comprehensive overview of various kinds of colloidal quantum dots, synthesized primarily as sub-20 nm spherical NCs, can be found in selected review articles [9, 12, 29, 37, 38]. Typical transmission electron microscopy (TEM) images of monodisperse, single-phase NCs are illustrated in Figure 1.4.

The success of the colloidal synthesis is mainly derived from (i) the virtually unlimited combinations of solvents–precursors–surfactants and (ii) the low temperature of the reactions and crystal growth, typically ranging from the room temperature to 350 °C. The low-temperature chemistry allows access to many far-from-equilibrium

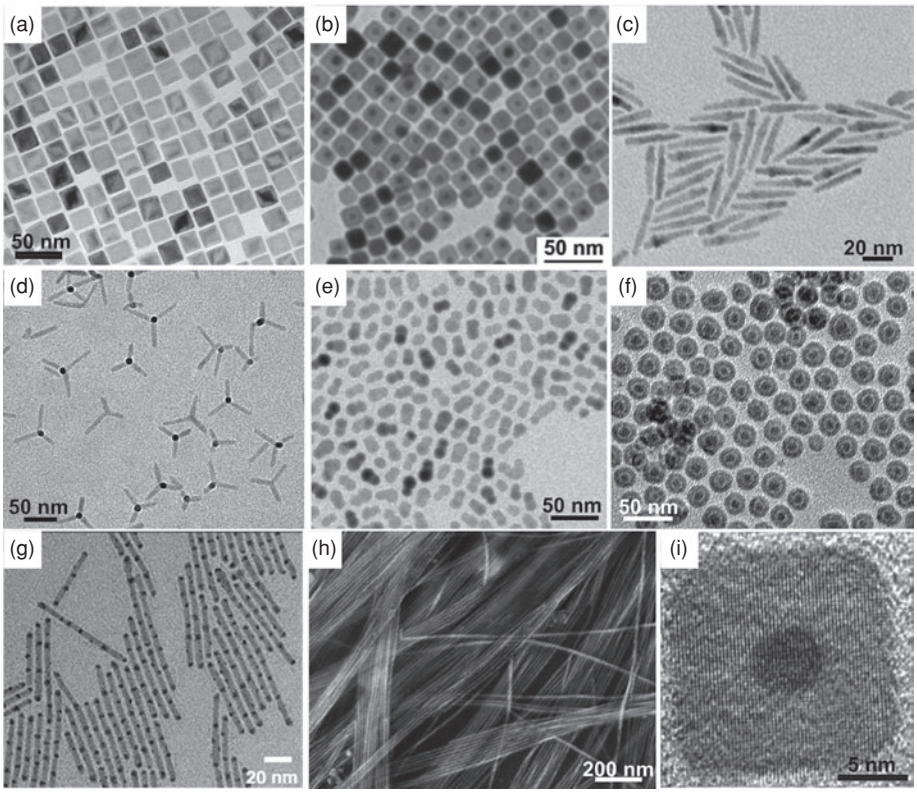

Figure 1.5 TEM images of: (a) 25 nm $Fe_xO/ZnFe_2O_4$ NCs; used with permission from [46]; (b) cubic Au/PbS NCs; used with permission from [47]; (c) CdSe/CdS nanorods; used with permission from [48]; (d) CdSe/CdS nanotetrapods; (e)$CoPt_3$/Au dumbbells; (f) gold/iron oxide (core/hollow-shell) NCs; (g) CdS/Ag_2S nanorods; used with permission from [49]. (h) SEM image of PbSe nanowires. (i) A high-resolution TEM image of FePt/PbS cubical core-shell NCs; used with permission from [50].

and metastable compositions and morphologies. Furthermore, the sought-after characteristics achievable with this method include precisely controlled size, size distribution, shape, and composition. Chemical methods opened access to an entirely new and previously inaccessible family of nanomaterials characterized by their complex shapes [39–42], compositional gradients, multicomponent architectures, and core–shell morphologies [37, 41, 43, 44]. Examples of multicomponent and shape-controlled NCs are shown in Figure 1.5. Importantly, colloidal methods are becoming increasingly inexpensive and robust. The synthetic equipment used is identical to the typical infrastructure for molecular chemistry, while inexpensive and simple precursors are converted into colloidal NCs with high atomic economy in just one or two steps. Furthermore, preparation and handling of nanoparticles in liquid phases is of paramount importance for occupational and environmental safety. Thermodynamically stable, clean and easy to handle colloidal solutions are ideal for low-temperature solution-based processes such as spin- and spray-coating, inkjet and screen printing [45].

The shape of the NC is determined by the interplay between the underlying crystal structure and the growth conditions. Thus, many different anisotropic shapes are found even in materials with highly symmetric crystal structures such as cubic rock-salt (e.g., IV–VI compounds), zinc-blende (most of the II–VI and III–V compounds) or face-centered cubic (fcc, many metals) lattices. In practice, efficient shape control is usually achieved through the selective adhesion of capping molecules to tune the crystal growth kinetics of different facets, leading to various faceted and anisotropic NCs (cubes, rods, wires, etc.) [39]. As an example, synthesis in a mixture of TOPO and alkylphosphonic acids (with varying length of alkyl chain) allows selective growth of the rod-, arrow-, rice-, teardrop-, and tetrapod-shaped CdSe NCs [42, 51]. There are multiple other phenomena that can be used to deliberately control the NC shape. The formation of single- and five-fold twin planes in fcc lattice of noble metal particles (Au, Ag) gives rise to nanorods and nanowires [52]. The observation of rod- and tetrapod-shaped Cd chalcogenide NCs is attributed to the polymorphism of the initial seeds – wurzite or zinc-blende [51]. Long and uniform colloidal nanowires can be synthesized by the oriented attachment and fusion of individual NCs [53] or via solution–liquid–solid [54] growth catalyzed by droplets of molten metallic nanoparticles (Au, Bi). Since the NC dimensions are comparable to the typical width of the reaction zone in solid-state reactions a number of unique growth modes have been found. The formation of hollow NCs was explained by the nanoscale Kirkendall effect – faster outward diffusion of atoms during the interfacial chemical reaction leading to the accumulation of vacancies [55]. In a confined space such as an NC, aggregation of vacancies forms a single hole, as observed during oxidation or sulfidation of Fe and Co NCs [56]. The cation exchange reactions were found to occur nearly instantly with the full preservation of the NC shape and size, allowing conversion of Cd-chalcogenide NCs to Pb- or Ag-chalcogenide NCs and vice-versa [57]. Similar hollow structures form with galvanic displacement reactions of Ag nanocubes with Au^{3+} ions [58, 59]. In this case, the void is formed because each Au^{3+} ion requires the oxidative dissolution of three silver atoms from the NC core.

The steep learning curve in the synthetic art and the rapid progress in atomic-level characterization techniques (e.g., aberration-corrected electron microscopy) lead one to expect further improvements of NC building blocks, and extension to previously inaccessible, yet highly technologically important, colloidal nanomaterials such as GaAs, many metallic alloys, and complex metal oxides.

1.2 Long-range ordered NC solids

1.2.1 Single-component NC superlattices

The great uniformity of sizes and shapes obtained has led to one of the most fascinating directions in NC research – the assembly of NCs into long-range ordered structures (superlattices, supercrystals). NC superlattices can spontaneously form upon the evaporation of the solvent. Just like atoms, monodisperse spherical particles pack into

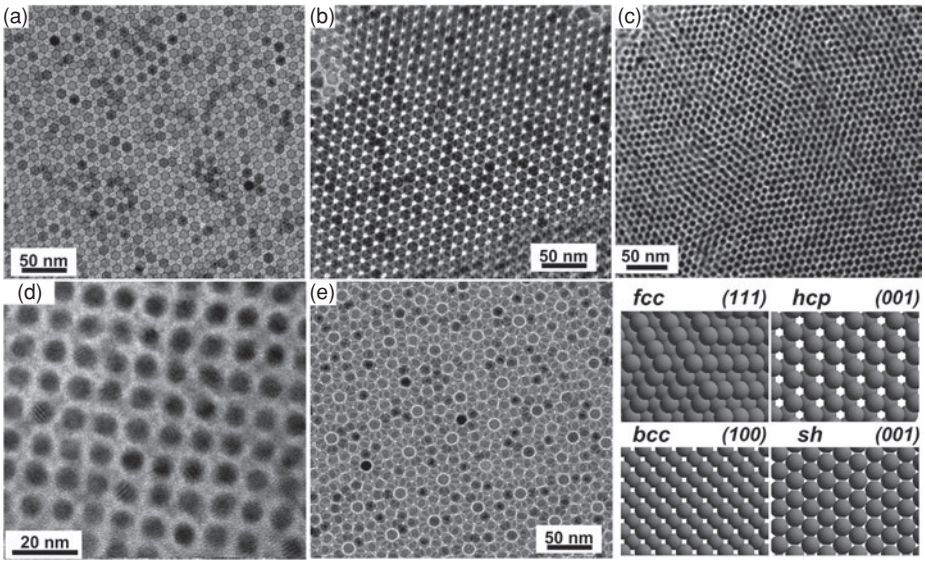

Figure 1.6 TEM images of (a) face-centered cubic and (b) hexagonal close-packed lattices formed by 11 nm $Fe_xO/CoFe_2O_4$ NCs. (c) The simple hexagonal lattice self-assembled from 7.2 nm PbSe NCs. Used with permission from [70]. (d) Body-centered cubic lattice self-assembled from 9 nm PbSe NCs. Used with permission from [71]. (e) Non-close-packed structures self-assembled from solution of 11 nm $Fe_xO/CoFe_2O_4$ NCs. Used with permission from [102].

dense crystalline structures, leading to a new class of materials – metamaterials or "artificial solids".

The packing of objects is one of the most ubiquitous phenomena and challenging problems in the materials world. Packing density in ordered structures is a central principle in the field of intermetallic compounds [60], liquid crystals [61], gem opals [62, 63], and also NCs [64]. NCs can arrange into two- and three-dimensional superlattices (Figures 1.6, 1.7). Very often they behave as hard (non-interacting) spheres, similarly to micron-sized silica or latex spheres [65, 66]. The hard-sphere approximation predicts the formation of ordered assemblies with the highest entropy. For example, monodisperse NCs typically pack into hexagonal close-packed (hcp) and fcc superlattices, which are known as the structures with the highest packing density of 0.74 for single-sized spherical particles. Entropy can favor the ordered state because of the increased local free space available for each sphere in the fcc lattice compared with the disordered state [67]. Theoretical calculations suggest that the fcc structure is slightly more stable than the hcp structure [68, 69], although the free energy difference is just $\sim 10^{-3} k_B T$ per particle. These structures differ only in how the hexagonal two-dimensional sheets of NCs stack on top of each other (Figure 1.6). Furthermore, there are many non-close-packed structures observed in NC superlattices (Figures 1.6(c)–(e)), which can only be explained as a result of strong interparticle interactions.

The self-assembly of NCs can occur both on solid substrates and at liquid surfaces and interfaces. The approaches to growing NC superlattices can be divided into two

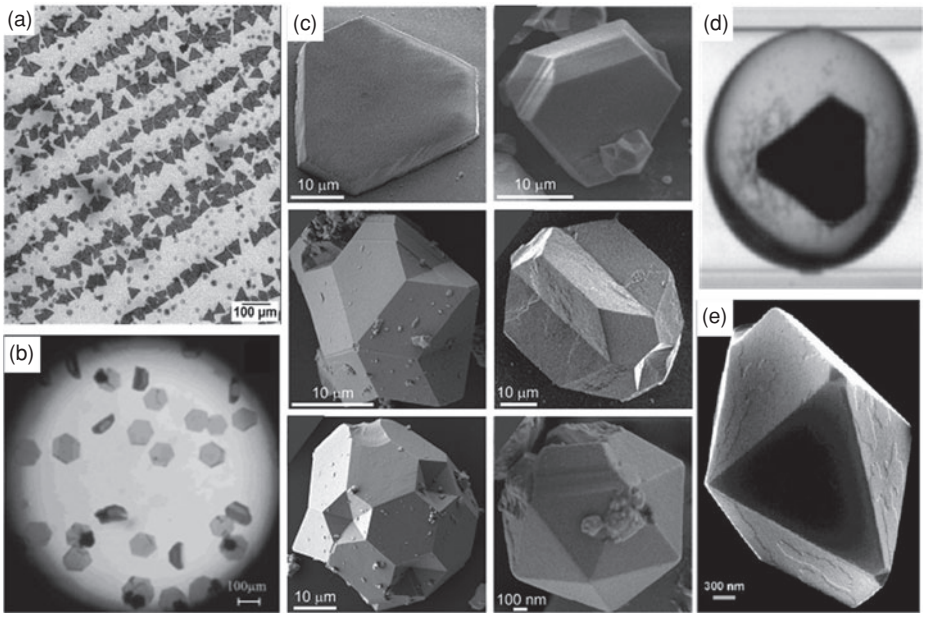

Figure 1.7 (a) Optical micrograph of three-dimensional colloidal crystals of 5.7 nm CdSe NCs. Used with permission from [9]. (b) Optical micrographs of colloidal crystals of CdSe NCs. Used with permission from [72]. (c) Scanning electron microscope (SEM) images showing the characteristic morphologies for superlattices self-assembled from PbS NCs of different sizes. Used with permission from [73]. (d) Optical image of the plug containing faceted superlattice of 11 nm $CoFe_2O_4$ NCs grown in nanoliter microfluidic plugs. Used with permission from [74]. (e) SEM image of faceted superlattice assembled from $CoPt_3$ NCs by the technique of controlled oversaturation. Used with permission from [75]. Color version of this figure is available online at www.cambridge.org/9780521198264.

categories. In "evaporation-driven" methods, the carrier solvent is slowly evaporated from a colloidal solution of NCs. When the NC volume fraction reaches a certain threshold, the system undergoes a transition from a disordered state to an ordered one, followed by the complete evaporation of the solvent. In contrast, "destabilization-driven" approaches use slow destabilization of a colloidal solution, typically achieved by layering the NC solution with a precipitant that slowly diffuses into the NC solution. It allows the growth of large three-dimensional faceted crystals (supercrystals, colloidal crystals) of long-range-ordered NCs. This approach is similar to the technique of free interface diffusion employed in protein crystallization [76] and has been successfully used for growing faceted three-dimensional superlattices of CdSe [9, 72], PbS [73, 77], FePt [78], $CoPt_3$ [75], Bi [30], and many other NCs.

1.2.2 Multicomponent NC superlattices

Binary NC superlattices (BNSLs)

The formation of binary crystals through self-assembly of larger and smaller particles (such as silica and latex spheres) has led to much interest in materials science since

the early 1980s [62, 63, 79, 80]. In 1990, this research was extended to nanomaterials: BNSLs were first observed for Au and Ag NCs of two different sizes [81, 82]. In 2002, small regions with AB_5 arrangement were found by Shevchenko *et al.* using mixtures of smaller and larger $CoPt_3$NCs [83]. Redl *et al.* extended this approach to NCs of two different compositions – binary NC superlattices isostructural with AB_2, AB_5 or AB_{13} compounds were formed from mixtures of semiconducting PbSe NCs and magnetic γ-Fe_2O_3NCs [84]. Shevchenko and coworkers have demonstrated the formation of BNSLs with AB, AB_2, AB_3, AB_4, AB_5, AB_6, and AB_{13} compositions, which are nanosize analogues of known ionic, atomic, and intermetallic phases (NaCl, CuAu, AlB_2, $MgZn_2$, $MgNi_2$, Cu_3Au, Fe_4C, $CaCu_5$, CaB_6, and $NaZn_{13}$) [85, 86]. Typical TEM images of such superlattices grown as thin films on carbon substrates are shown in Figure 1.8.

The details of the crystallography [87–89], thermodynamics [90], and kinetics [91] of NC assembly have attracted broad interest in the scientific community. Many key features of conventional atomic and molecular crystals, such as faceting, twinning, polymorphism, etc. have been observed in NC superlattices [73, 92–94]. Major efforts are focused on understanding the self-organization of NCs [89, 95, 96] and developing robust methods for large-area self-assembly. Centimeter-scale, uniform membranes of BNSLs that can readily be transferred to arbitrary substrates have been prepared by the liquid–air interfacial assembly of NCs [97].

Studies of binary NC superlattices have shown that entropy often dominates the assembly of sterically stabilized NCs [64, 95]. The gain in free volume entropy upon ordering of hard spheres is greater than the decrease in configurational entropy, thus providing a net positive change in the system's entropy. This purely entropic effect favors the formation of highly dense NC superlattices with AlB_2, $NaZn_{13}$, and NaCl structure, whose packing densities can be higher than single-component lattices (fcc or hcp). The packing density (ρ) in the BNSL is a function of the effective size ratio (γ_{eff}) between smaller and larger NCs, as illustrated by so-called space-filling curves (Figure 1.8). This implies that the size ratio is an important consideration for obtaining BNSL with a certain structure. Densely packed AlB_2- and $NaZn_{13}$-type lattices are found in natural as well as artificial opals built of (sub)micrometer spheres [79]. However, other BNSLs form at packing densities much lower than single-component fcc or hcp structures, yet they are stable against phase separation into individual lattices. The stability of these BNSLs can be explained by the contribution from the entropy of mixing and additional configurational entropy. In addition, contributions from particle–particle and particle–substrate interactions such as Coulombic, van der Waals, charge–dipole, dipole–dipole, entropic, capillary, convective, shear, and other forces have been widely discussed [98]. Finally, van der Waals ligand–ligand interactions between long hydrocarbon ligands are also important [70, 99]. At the nanoscale, the magnitudes of all these interactions are often comparable to each other, providing flexibility to the interparticle potentials [100]. Assuming near-equilibrium conditions for NC self-assembly, the change in the Gibbs free energy can be generally expressed as $dG = dH - TdS$ [101]. All specific interparticle interactions can be grouped into the enthalpy term dH, whereas packing principles contribute to the entropic term TdS. Accordingly, temperature can determine